



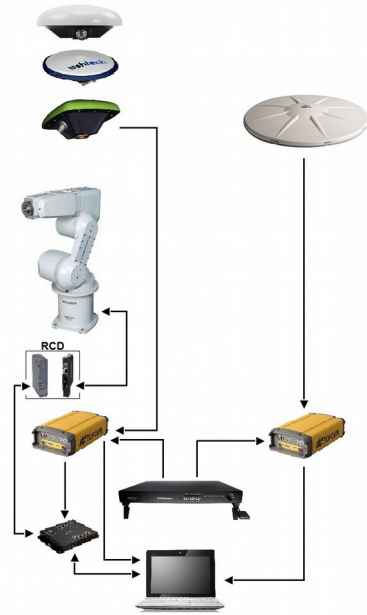
INDIVIDUAL CALIBRATION ANTENNA PCC MODELS: DIFFERENCES AND THEIR IMPACT ON TROPOSPHERIC ESTIMATES: LEIAR25 CASE STUDY

Grzegorz Krzan, Katarzyna Stępniaik
Institute of Geodesy, University of Warmia and Mazury in Olsztyn, Poland
ul. Oczapowskiego 1, 10-720 Olsztyn
grzegorz.krzan@uwm.edu.pl



Motivation

- study connected with GRAVER project focused on the development and implementation of field calibration procedure for multi-frequency and multi-system GNSS antennas
- preparation for antenna calibration for receiving new signals from developed and modernized GNSS constellations
- develop the method of verification and validation of calibration results
- investigate the impact of differences in GNSS antenna calibrations models on the quality of the tropospheric estimate series for climate applications;



Comparison of robot and chamber calibration techniques

Robot calibration (GEO++)

- uses **real satellite signals** in the natural environment, taking into account signal strength and all disturbing effects
- it is usable **only for available signals**;
- **strong multipath** from surrounding objects, so more demanding post-processing needed to mitigate;
- **long duration** of observation
- **variable** environment

Anechoic chamber calibration (UniBonn)

- uses „**artificial**” **signal** in the form of generated sine wave
- any frequency available to calibrate;
- **weak multipath** effect
- **short duration** of observation
- **stable** environment

Data and Method

- data collected at **19 EPN stations** were processed with **NAPEOS** software;
- PPP and Zero-differenced network solution utilizing **ESA** precise satellite **orbits and clocks** were used;
- The first solution was obtained by applying the **IGS type-mean** Phase Center Correction (PCC) models. In the second and third solutions PCC models from **individual field robot calibration and calibration in anechoic chamber** were used;
- All three solutions were processed several times – using **GPS only**, **GPS+GLONASS**, **GPS+Galileo** and **multi-GNSS** (GPS+GLONASS+Galileo) observations;
- In order to validate and assess the quality of the GNSS solutions, tropospheric estimates obtained from solutions were compared to **ERA-Interim** reanalysis derived ZTDs.



Detailed parameters of solutions.

| | | |
|----------------------------|--|---|
| Processing variant | Standard Precise Point Positioning (PPP) | Zero-differenced network solution |
| Utilized GNSS systems | GPS-only GPS+GLONASS GPS+GLONASS+Galileo | GPS-only GPS+Galileo |
| Basic observables | | Undifferenced carrier phases & pseudoranges; |
| Processed time span | 1Y 2017 | 2Y 2017-18 |
| Phase ambiguity fixing | Float ambiguities solution | Fixed ambiguities solution |
| Orbit & clock products | | ESA precise final orbit and clock (30 s) products; |
| Ionospheric delay | | 1st order effect: accounted for dual frequency ionosphere-free linear combination; 2nd order effect: no corrections applied; |
| Tropospheric delay | Zenith dry delay computed using the Saastamoinen model with pressure and temperature from the GPT model; the resulting zenith delay is mapped using the dry GMF mapping function; Wet delay estimated using the wet GMF mapping function; Tropospheric estimates computed with 1h interval | |
| Ocean loadings | | Computed for FES2004 model using ONSALA ocean loading service; |
| Tidal displacement | | In accordance with IERS2010 (Petit and Luzum 2010); |
| Satellite clock correction | | 2nd order relativistic correction for non-zero orbit ellipticity ($-2 \cdot R \cdot V / c$) applied; |
| Observation weighting | | Carrier phase: 10 mm sigma (for zenith); Pseudorange: 1 m sigma (for zenith); Sigmas increase with increasing zenith angle using the function $(1 / \cos(z))$; |
| Others | | Observation sampling rate: 5 minutes Elevation angle cut-off 5° |
| | Antenna PCC models: IGS14 type-mean calibration, individual robot calibration, individual chamber calibration | |



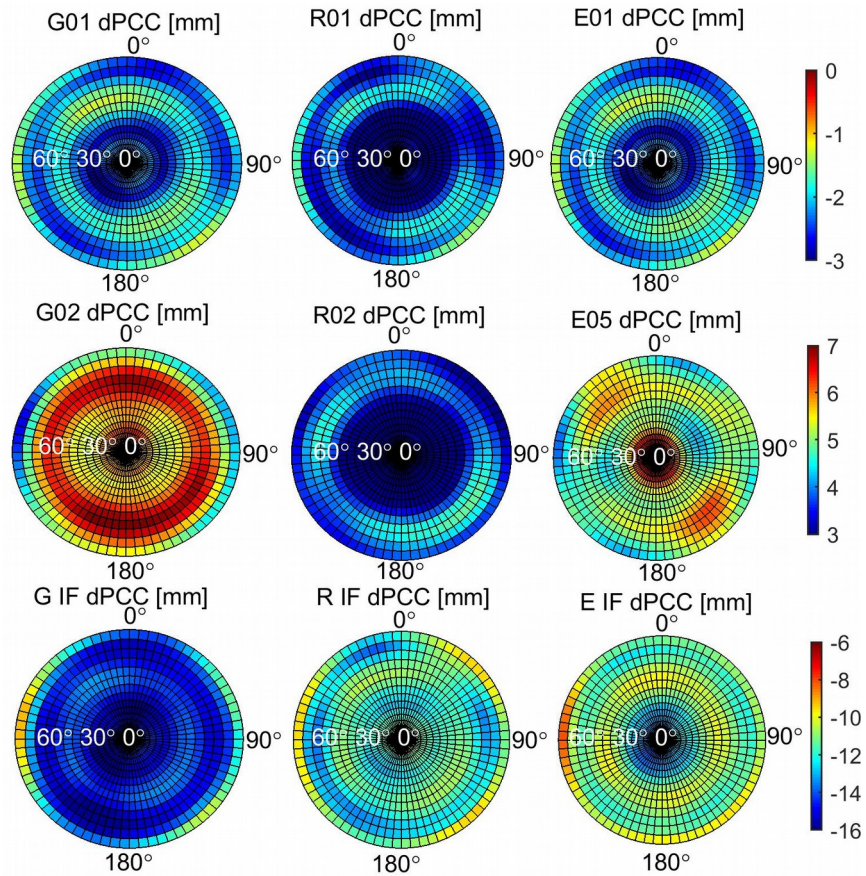
Hardware characteristics of the test stations

| No. | Station | Network | Station hardware | |
|-----|---------|---------|-----------------------------------|----------------------|
| | | | Antenna type | Receiver type |
| 1 | AUBG | EPN | LEIAR25.R4 LEIT | LEICA GR25 |
| 2 | BORJ | EPN | LEIAR25.R3 LEIT | JAVAD TRE_3 DELTA |
| 3 | DIEP | EPN | LEIAR25.R4 LEIT | LEICA GR25 |
| 4 | DILL | EPN | LEIAR25.R4 LEIT | LEICA GR25 |
| 5 | DOUR | EPN | LEIAR25.R3 NONE | SEPT POLARX4 |
| 6 | EUSK | EPN | LEIAR25.R4 LEIT | LEICA GR25 |
| 7 | GELL | EPN | LEIAR25.R4 LEIT / LEIAR25.R3 LEIT | LEICA GR25 |
| 8 | GOR2 | EPN | LEIAR25.R4 LEIT | LEICA GR25 |
| 9 | HEL2 | EPN | LEIAR25.R3 LEIT | LEICA GR25 |
| 10 | HELG | EPN | LEIAR25.R4 LEIT | JAVAD TRE_G3TH DELTA |
| 11 | HOFJ | EPN | LEIAR25.R4 LEIT | LEICA GR25 |
| 12 | ISTA | EPN | LEIAR25.R4 LEIT | LEICA GR25 |
| 13 | KARL | EPN | LEIAR25.R4 LEIT | JAVAD TRE_3 DELTA |
| 14 | LDB2 | EPN | LEIAR25.R4 LEIT | LEICA GR25 |
| 15 | LEIJ | EPN | LEIAR25.R3 LEIT | JAVAD TRE_G3TH DELTA |
| 16 | RANT | EPN | LEIAR25.R4 LEIT | JAVAD TRE_G3TH DELTA |
| 17 | SAS2 | EPN | LEIAR25.R4 LEIT | JAVAD TRE_G3TH DELTA |
| 18 | WARN | EPN | LEIAR25.R3 LEIT | JAVAD TRE_G3TH DELTA |
| 19 | WRLG | EPN | LEIAR25.R3 LEIT | LEICA GR25 |

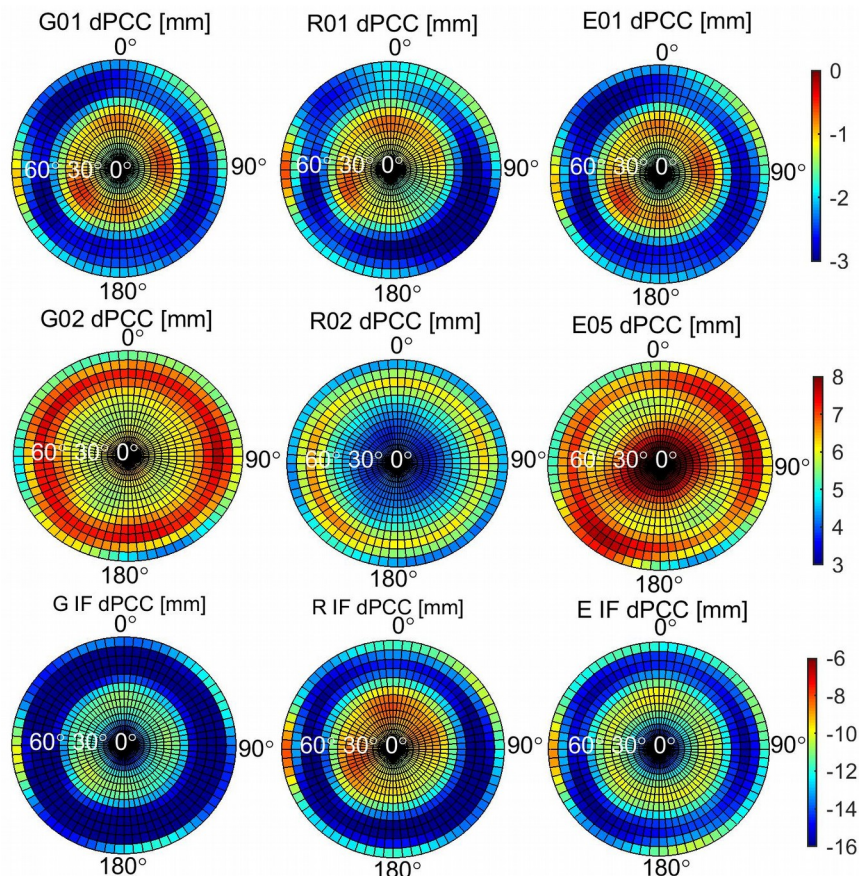


Azimuth and elevation dependent PCC differences obtained by comparison of chamber and

DOUR LEIAR25.R3 NONE



HELG LEIAR25.R4 LEIT



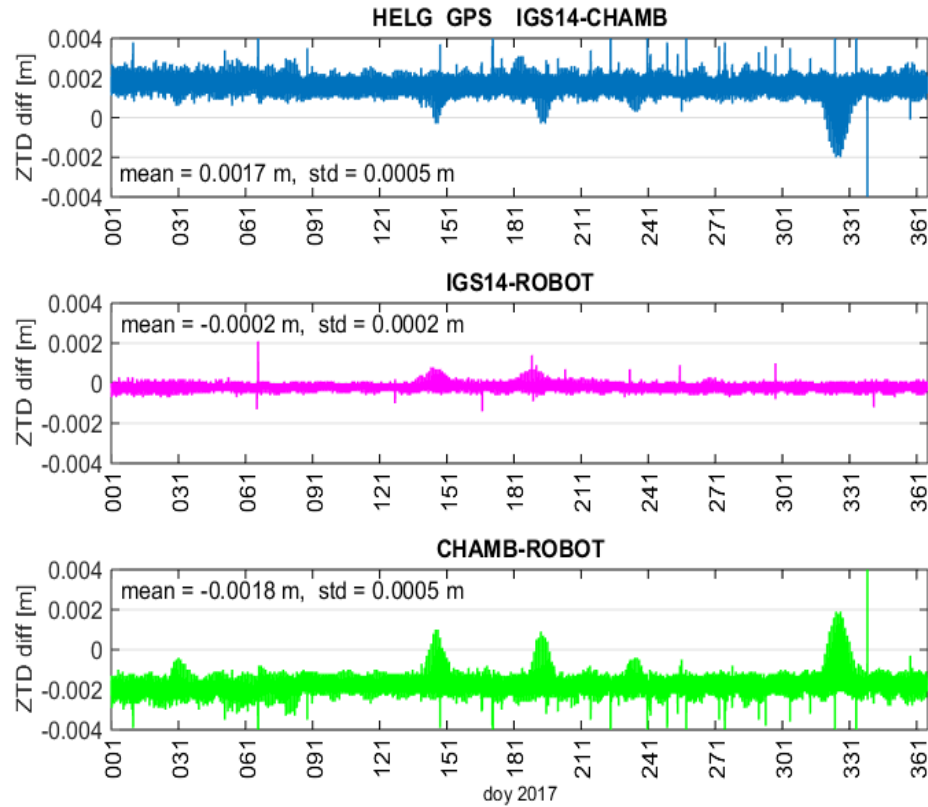
dPCC within the same azimuth:

- L1: max 4 mm
- L2: max 10 mm
- IF: max 20 mm

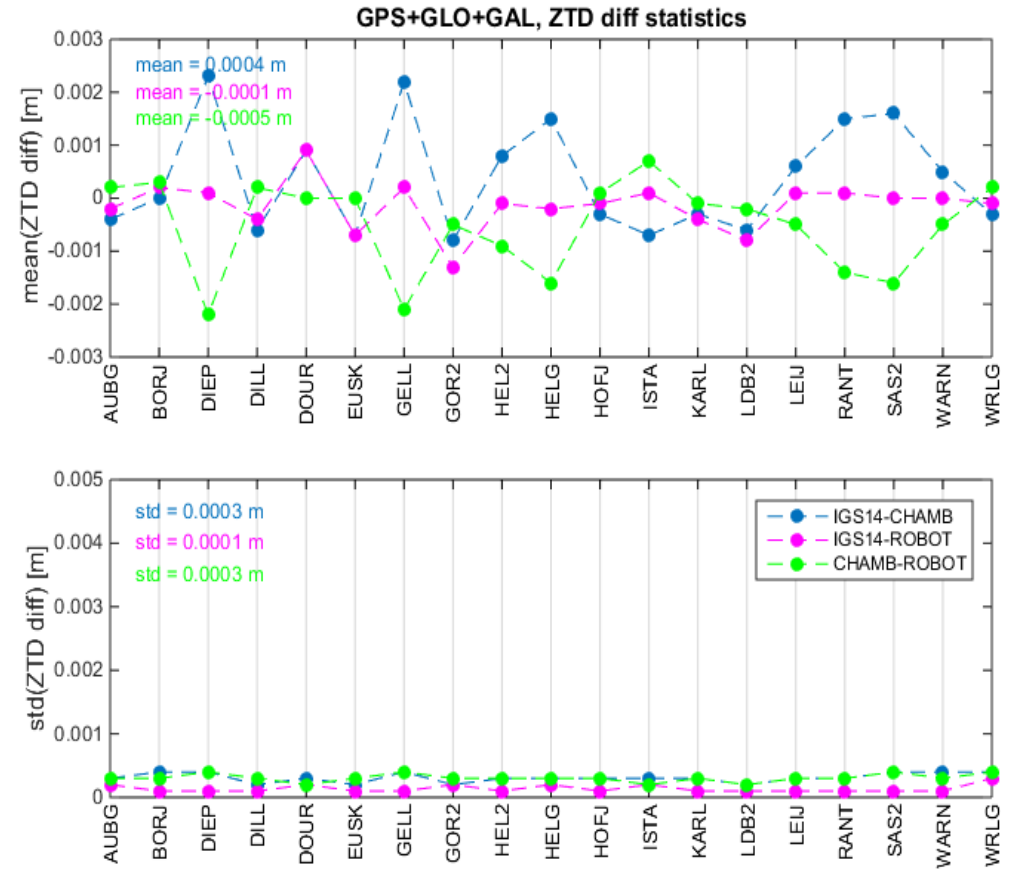
dPCC within the same zenith angle:

- L1: max 3 mm
- L2: max 3 mm
- IF: max 5 mm

Standard PPP solution:



Time series of ZTD differences for station HELG; GPS-only processing.



Mean and standard deviation of ZTD differences between variants for GPS+GLO+GAL processing for 19 stations over 1 year of data.



Statistics of ZTD differences for 3 selected stations. Differences between antenna calibration variants for GPS-only, GPS+GLONASS and GPS+GLONASS+Galileo processing

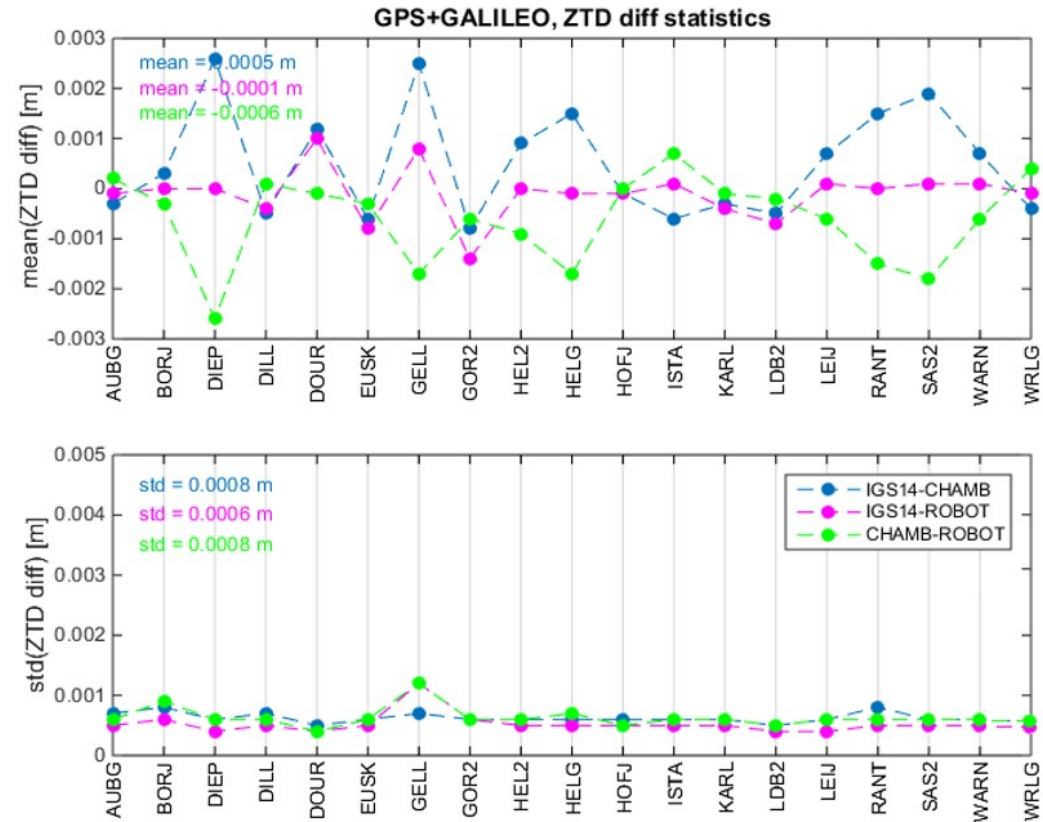
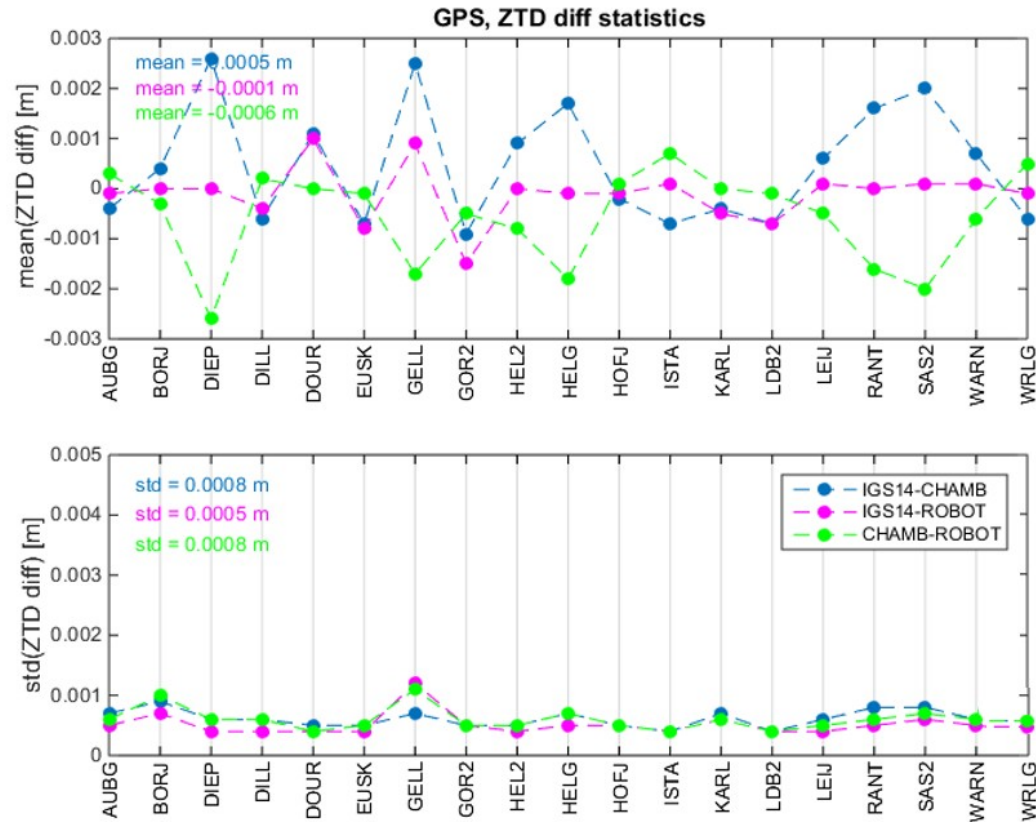
| Data/System | GPS | | | [GPS+GLO] | | | [GPS+GLO+GAL] | | |
|--------------------|-------------|-------------|-------------|-------------|-------------|-------------|---------------|-------------|-------------|
| Calibration model | IGS14-CHAMB | IGS14-ROBOT | CHAMB-ROBOT | IGS14-CHAMB | IGS14-ROBOT | CHAMB-ROBOT | IGS14-CHAMB | IGS14-ROBOT | CHAMB-ROBOT |
| | | DILL | | | DILL | | | DILL | |
| mean(ZTD diff) [m] | -0.0005 | -0.0003 | 0.0002 | -0.0007 | -0.0004 | 0.0003 | -0.0006 | -0.0004 | 0.0002 |
| std(ZTD diff) [m] | 0.0002 | 0.0001 | 0.0003 | 0.0002 | 0.0003 | 0.0004 | 0.0002 | 0.0001 | 0.0003 |
| | | HELG | | | HELG | | | HELG | |
| mean(ZTD diff) [m] | 0.0017 | -0.0002 | -0.0018 | 0.0015 | -0.0002 | -0.0017 | 0.0015 | -0.0002 | -0.0016 |
| std(ZTD diff) [m] | 0.0005 | 0.0002 | 0.0005 | 0.0005 | 0.0002 | 0.0005 | 0.0003 | 0.0002 | 0.0003 |
| | | KARL | | | KARL | | | KARL | |
| mean(ZTD diff) [m] | -0.0004 | -0.0004 | -0.0001 | -0.0004 | -0.0004 | 0.0000 | -0.0003 | -0.0004 | -0.0001 |
| std(ZTD diff) [m] | 0.0003 | 0.0001 | 0.0003 | 0.0003 | 0.0001 | 0.0003 | 0.0003 | 0.0001 | 0.0003 |

Statistics of ZTD differences for 3 selected stations. Differences between data variants

| Calibration model | IGS14 | CHAMB | ROBOT |
|--------------------|---------|-------------|---------|
| Data/System | | DILL | |
| mean(ZTD diff) [m] | -0.0007 | -0.0008 | -0.0007 |
| std(ZTD diff) [m] | 0.0020 | 0.0021 | 0.0019 |
| | | HELG | |
| mean(ZTD diff) [m] | 0.0000 | -0.0002 | -0.0001 |
| std(ZTD diff) [m] | 0.0130 | 0.0133 | 0.0130 |
| | | KARL | |
| mean(ZTD diff) [m] | 0.0000 | -0.0001 | 0.0000 |
| std(ZTD diff) [m] | 0.0014 | 0.0014 | 0.0014 |

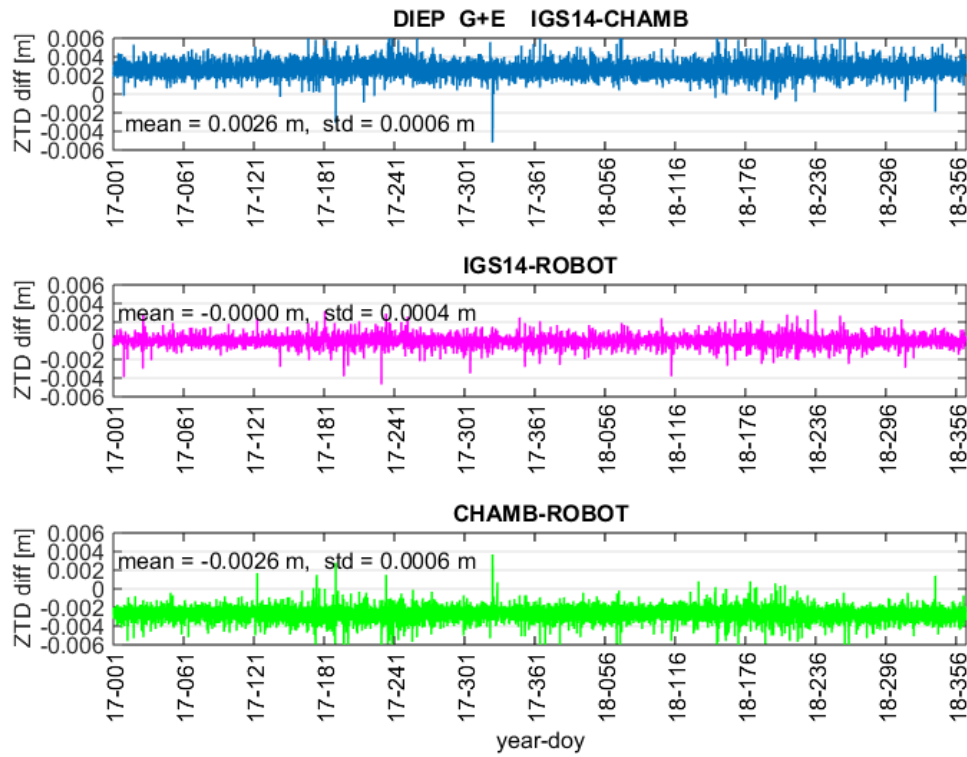


Zero-differenced network solution (2017-2018):

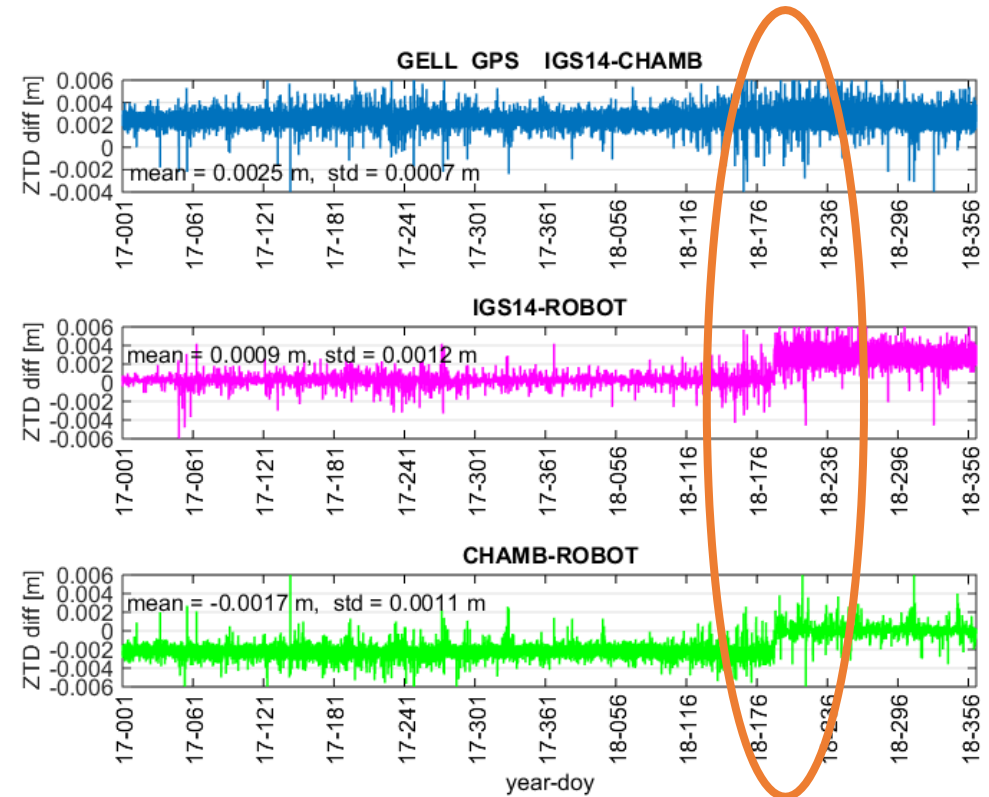


Mean and standard deviation of ZTD differences between variants for GPS only processing (left) and GPS+Galileo processing (right) over 2 years of data.

Zero-differenced network solution (2017-2018):

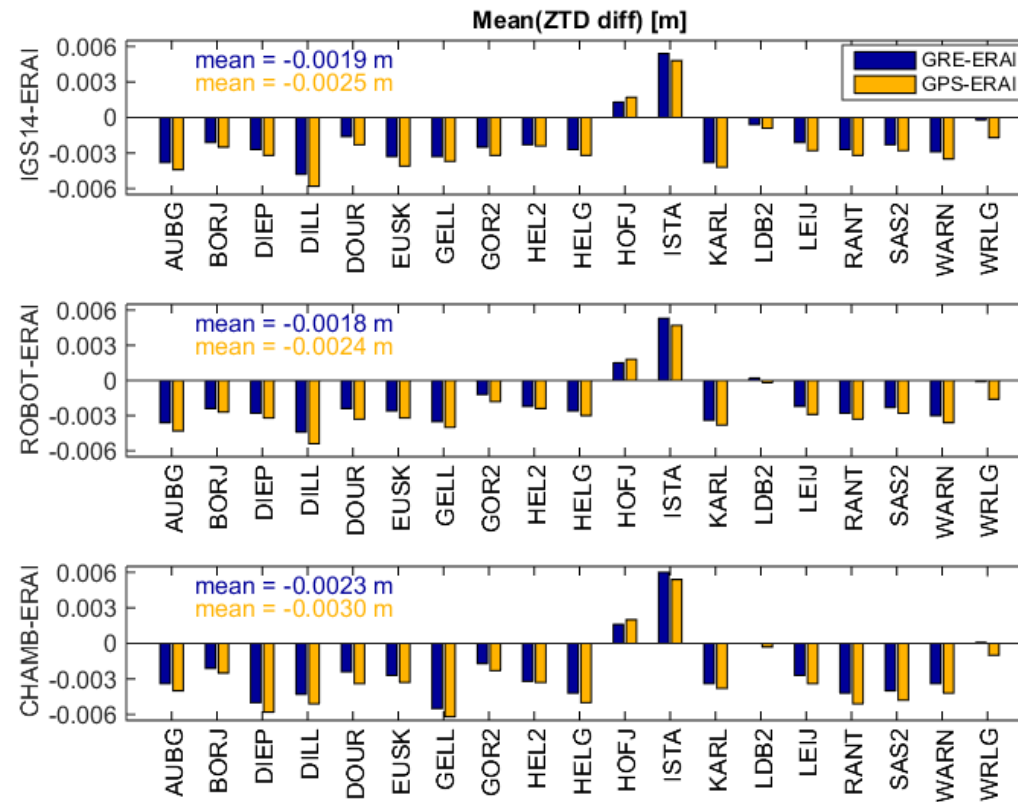


Time series of ZTD differences for station DIEP, GPS+Galileo processing.



Time series of ZTD differences for station GELL, GPS processing.

Mean ZTD differences between PPP [GPS+GLO+GAL] solution and ERA-Interim (navy blue) as well as ZD network solution (GPS-only) and ERA-Interim (orange), for 2017.



Summary and conclusions

- Overall, the mean standard deviation of **ZTD differences is higher for differences between variants using observations from different satellite systems** than for variants using different antenna calibration models. However, the impact of applying individual calibrations is not negligible. The results depend on the equipment (receiver and antenna) of the stations;
- Validation against data from climate reanalysis confirms that **all approaches provide high-quality tropospheric delays**;
- The mean bias between ZTD from GNSS processing and ERA-Interim depends on the processing options (antenna model calibration) and varies from -6.2 mm to -0.2 mm, except two stations: ISTA and HOFJ with the bias 5.6 mm and 1.8 mm respectively. Negative mean ZTD bias for almost all comparisons suggests that ZTDs achieved from the ERA Interim reanalysis are drier than those obtained from GNSS reprocessing. For stations ISTA and HOFJ the reason of positive mean ZTD bias between GNSS and ERA-Interim needs further investigation.
- Based on the mean ZTD differences, it can be concluded that **[GPS+GLO+GAL] processing variant is closer to ERA-Interim than GPS only processing variant**. At the same time, ZTD estimates obtained from variants using **ROBOT and IGS14 calibration are also slightly closer to estimated from ERA-Interim** than estimates from variant with calibration in anechoic chamber.





INDIVIDUAL CALIBRATION ANTENNA PCC MODELS: DIFFERENCES AND THEIR IMPACT ON TROPOSPHERIC ESTIMATES: LEIAR25 CASE STUDY

Grzegorz Krzan, Katarzyna Stępniaak
Institute of Geodesy, University of Warmia and Mazury in Olsztyn, Poland
ul. Oczapowskiego 1, 10-720 Olsztyn
grzegorz.krzan@uwm.edu.pl

